

Color-Tuned Highly Fluorescent Organic Nanowires/ Nanofabrics: Easy Massive Fabrication and Molecular Structural Origin

Byeong-Kwan An, Se Hoon Gihm, Jong Won Chung, Chong Rae Park,*
Soon-Ki Kwon,[†] and Soo Young Park*

Department of Materials Science and Engineering, ENG445, Seoul National University, San 56-1, Shillim-dong, Kwanak-ku, Seoul 151-744, Korea, and Department of Polymer Science and Engineering and Research Institute of Industrial Technology, Gyeongsang National University, Jinju 660-701, Korea

Received August 6, 2008; E-mail: parksy@snu.ac.kr; cnpark@snu.ac.kr

Abstract: The development of one-dimensional fluorescent nanowires (1D-NWs) and their higher-dimensional architectures such as nanowebs and nanofabrics (2D-NFs) could open a new area in nanomaterials science and nanotechnology. In particular, fluorescent π -electronic 1D-NWs are considered promising materials for realizing innovative nanodevices together with semiconductors and metallic NWs. We earlier reported that 1-cyano-*trans*-1,2-bis-(3',5'-bis-trifluoromethyl-biphenyl)ethylene (CN-TFMBE), a simple but very peculiar derivative of oligo(*p*-phenylene vinylene)s (OPV) composed of a cyano-stilbene backbone, self-assembles easily into 1D-NWs with highly enhanced fluorescence emission in the solid state. We report herein surprising new outcomes obtained from a more detailed exploration of the self-association behavior of CN-TFMBE and its analogues. We found that CN-TFMBE self-assembled into highly fluorescent 1D-NWs and 2-D NFs very easily and massively, irrespective of whether drop casting, spin coating, or vacuum deposition was used for processing. However, we additionally found that, if the backbone cyano group or trifluoromethyl substituents were removed from CN-TFMBE, the resulting molecule did not form 1D-NWs under any conditions. Through structural analyses using mid- and wide-angle X-ray diffraction methods and multiscale computer simulation techniques, we formulated molecular structural guidelines for programming π -electron molecules into highly fluorescent 1D-NWs and 2-D NFs. Interestingly, we demonstrated that R,G,B,Y-color tuned 1D-NWs and NFs could be easily and massively fabricated based on our guidelines. This class of highly fluorescent color-tuned organic π -electronic nanomaterial is expected to open a new phase in applications such as nanoscale optoelectronics, sensing, and biological devices.

Introduction

One-dimensional fluorescent nanowires (1D-NWs) of π -conjugated organic molecules^{1–3} have been fascinating scientists because they open up new possibilities such as nanoscale biological and optoelectronic devices over a wide range of fluorescent semiconductors^{4–7} and metallic 1D-NWs.^{8,9} In particular, fluorescent organic 1D-NWs are expected to have distinctive advantages over fluorescent semiconductors and metallic 1D-NWs, such as diversity and flexibility in material selection, low-cost in situ fabrication via self-assembly, high-

volume production, and comparatively easy control of optoelectrical properties.^{1,10} However, fabricating tailor-made highly fluorescent 1D-NWs with optimal optoelectronic properties has proved a great challenge. This is due, on the one hand, to a lack of clear guidelines for the design of molecular structures that induce self-assembly into 1D architectures such as 1D-NWs, and, on the other hand, to the concentration-fluorescence-quenching phenomenon that occurs when fluorescent organic molecules aggregate.

We have recently reported that 1-cyano-*trans*-1,2-bis-(3',5'-bis-trifluoromethyl-biphenyl)ethylene (CN-TFMBE) molecules

[†] Gyeongsang National University.

- (1) (a) George, S. J.; Ajayaghosh, A. *Chem. Eur. J.* **2005**, *11*, 3217–3227. (b) Ajayaghosh, A.; Praveen, V. K. *Acc. Chem. Res.* **2007**, *40*, 644–656. (c) Herrikhuyzen, J. V.; George, S. J.; Vos, M. R. J.; Sommerdijk, N. A. J. M.; Ajayaghosh, A.; Meskers, S. C. J.; Schenning, A. P. H. J. *Angew. Chem., Int. Ed.* **2007**, *46*, 1825–1828. (d) Ajayaghosh, A.; Praveen, V. K.; Vijayakumar, C. *Chem. Soc. Rev.* **2008**, *37*, 109–122.
- (2) Chen, Y.; Chen, X.; Li, B.; Yu, D.; He, Z.; Li, G.; Zhang, M. *Appl. Phys. Lett.* **2006**, *89*, 241121.
- (3) O'Carroll, D.; Lieberwirth, I.; Redmond, G. *Nat. Nanotechnol.* **2007**, *2*, 180–184.
- (4) Xia, Y. N.; Yang, P. D.; Sun, Y. G.; Wu, Y. Y.; Mayers, B.; Gates, B.; Yin, Y. D.; Kim, F.; Yan, Y. Q. *Adv. Mater.* **2003**, *15*, 353–389.
- (5) Cheng, B. C.; Wang, Z. G. *Adv. Funct. Mater.* **2005**, *15*, 1883–1890.

- (6) Hayden, O.; Payne, C. K. *Angew. Chem., Int. Ed.* **2005**, *44*, 1395–1398.
- (7) Nakayama, Y.; Pauzauskie, P. J.; Radenovic, A.; Onorato, R. M.; Saykally, R. J.; Liphardt, J.; Yang, P. D. *Nature* **2007**, *447*, 1098–1102.
- (8) Tok, J. B. H.; Chuang, F. Y. S.; Kao, M. C.; Rose, K. A.; Pannu, S. S.; Sha, M. Y.; Chakarova, G.; Penn, S. G.; Dougherty, G. *Angew. Chem., Int. Ed.* **2006**, *45*, 6900–6904.
- (9) Goldys, E. M.; Drozdowicz-Tomsia, K.; Xie, F.; Shtoyko, T.; Matveeva, E.; Gryczynski, I.; Gryczynski, Z. *J. Am. Chem. Soc.* **2007**, *129*, 12117–12122.
- (10) (a) Terech, P.; Weiss, R. G. *Chem. Rev.* **1997**, *597*, 3133–3159. (b) Hoebe, F. J. M.; Jonkheijm, P.; Meijer, E. W.; Schenning, A. P. H. J. *Chem. Rev.* **2005**, *105*, 1491–1546.

readily self-assemble into 1D-NWs during the course of organogelation,¹¹ and exhibit aggregation-induced enhanced emission (AIEE)^{12–19} instead of the notorious concentration fluorescence quenching phenomenon that is generally observed for π -electronic molecules.²⁰ Indeed, the CN-TFMBE molecule itself is inherently almost nonfluorescent in the isolated state but becomes highly fluorescent in the aggregated state, showing a more than 100-fold enhancement in fluorescence intensity. This behavior stands in striking contrast to conventional fluorescent materials. Another interesting feature of CN-TFMBE molecules is that they form 1D-NWs even though they lack long alkyl units on their backbone structure.

To achieve a detailed understanding of the unique features of CN-TFMBE molecules, we systematically explored the self-assembled structures and self-association behaviors of CN-TFMBE molecules and newly synthesized analogues. Furthermore, on the basis of our fundamental understanding of the molecular structural origins of the peculiar self-assembly into 1D-NWs and AIEE properties of CN-TFMBE, which were supported by analyses using mid- and wide-angle X-ray diffraction methods and multiscale computer simulation techniques, we successfully developed a method for producing large amounts of highly fluorescent R,G,B,Y-color tuned nanofabrics consisting of extremely uniform 1D-NWs.

Results and Discussion

Effect of Fabrication Conditions on the NW Self-Assembly of CN-TFMBE Molecules. To examine the effect of the fabrication method and conditions on the self-assembly of CN-TFMBE molecules into 1D-NWs, we investigated various fabrication methods including drop casting, recrystallization, and vacuum evaporation, as well as the spin coating of a mixture of a polymer matrix and CN-TFMBE followed by thermal annealing and/or solvent vapor-driven self-assembly. As illustrated in Figure 1, CN-TFMBE molecules readily self-assembled into highly fluorescent 1D-NWs irrespective of the fabrication method and conditions. However, the general characteristics of the 1D-NWs, such as the amount, diameter, and aspect ratio, were influenced by the fabrication method and conditions. Field emission scanning electron microscopy (FE-SEM) of the CN-TFMBE 1D-NWs generated by solution drop casting (0.2 wt % in 1,2-dichloroethane) (Figure 1a) disclosed that the 1D-NWs had an extremely high aspect ratio and were ~ 100 nm in diameter, with some NWs combining into bundles with micrometer-sized diameters. In addition, fluorescence

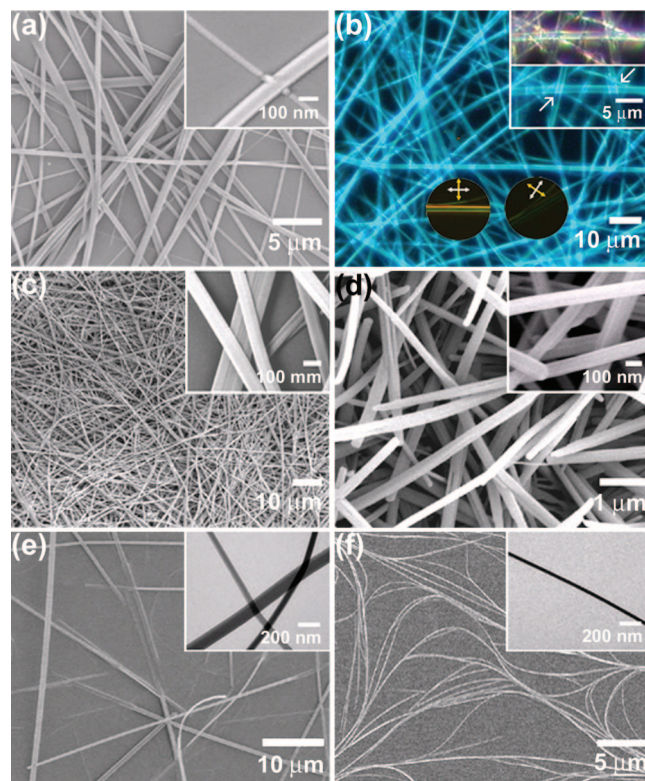


Figure 1. FE-SEM micrographs of self-assembled 1D nanowire structures of CN-TFMBE molecules (a) fabricated by drop casting using a 0.2 wt % solution of CN-TFMBE in 1,2-dichloroethane. (b) Fluorescence microscopy images of CN-TFMBE nanowires obtained by the method described in (a) (circular inset photos show the birefringence of the CN-TFMBE nanowire bundles under crossed polarizers). (c) Fabricated by recrystallization of a 0.5 wt % solution of CN-TFMBE in a methanol/1,2-dichloroethane (1:9 v/v) mixture. (d) Fabricated by vacuum evaporation and (e) by thermal annealing of a PMMA film spin coated using a 3.0 wt % CN-TFMBE (10.0 wt % with respect to PMMA) solution in 1,2-dichloroethane [(Inset) TEM image of the CN-TFMBE nanowires generated in situ in the PMMA film]. (f) Fabricated by methylene chloride vapor-driven self-assembly (VDSA) in a PMMA film (fabricated by the method described in (e)). [(Inset) TEM image of CN-TFMBE nanowires generated in situ in the PMMA film].

microscopy showed that the NWs produced by this method exhibited intense blue fluorescence owing to the AIEE phenomenon^{13–19} (Figure 1b); this stands in contrast to the behavior of isolated CN-TFMBE molecules in solution, which are almost nonfluorescent regardless of solvent polarity.¹¹ In particular, the self-assembled CN-TFMBE 1D-NWs are transparent; hence, when the CN-TFMBE 1D-NWs overlap, the fluorescence of underlying NWs is projected through the higher NWs (as indicated by arrows in the inset of Figure 1b). This effect can be attributed to the high crystallinity of the NWs, which also leads to strong birefringence under crossed polarizers (circled region in Figure 1b). A highly fluorescent CN-TFMBE 1D-NWs was also readily obtained by recrystallization of a 0.5 wt % CN-TFMBE solution in a methanol/1,2-dichloroethane (1:9 v/v) mixture (Figure 1c), and by vacuum evaporation (Figure 1d). Even when CN-TFMBE molecules were dispersed in a polymethyl methacrylate (PMMA) matrix, 1D-NWs of ~ 100 nm in diameter were readily generated in situ via either thermal annealing (Figure 1e) or a solvent (methylenechloride in this case) vapor-driven self-assembly (VDSA) process¹⁹ (Figure 1f). These observations thus indicate that CN-TFMBE molecules have an intrinsic propensity to form highly fluorescent 1D-NWs.

- (11) An, B. K.; Lee, D. S.; Lee, J. S.; Park, Y. S.; Song, H. S.; Park, S. Y. *J. Am. Chem. Soc.* **2004**, *126*, 10232–10233.
- (12) An, B. K.; Kwon, S. K.; Jung, S. D.; Park, S. Y. *J. Am. Chem. Soc.* **2002**, *124*, 14410–14415.
- (13) Luo, J. D.; Xie, Z. L.; Lam, J. W. Y.; Cheng, L.; Chen, H. Y.; Qiu, C. F.; Kwok, H. S.; Zhan, X. W.; Liu, Y. Q.; Zhu, D. B.; Tang, B. Z. *Chem. Commun.* **2001**, *18*, 1740–1741.
- (14) Lim, S. J.; An, B. K.; Jung, S. D.; Chung, M. A.; Park, S. Y. *Angew. Chem., Int. Ed.* **2004**, *43*, 6346–6350.
- (15) Bhongale, C. J.; Chang, C. W.; Lee, C. S.; Diau, E. W. G.; Hsu, C. S. *J. Phys. Chem. B* **2005**, *109*, 13472–13482.
- (16) Xie, Z. Q.; Yang, B.; Cheng, G.; Liu, L. L.; He, F.; Shen, F. Z.; Ma, Y. G.; Liu, S. Y. *Chem. Mater.* **2005**, *17*, 1287–1289.
- (17) An, B. K.; Kwon, S. K.; Park, S. Y. *Bull. Korean Chem. Soc.* **2005**, *26*, 1555–1559.
- (18) Tong, X.; Zhao, Y.; An, B. K.; Park, S. Y. *Adv. Func. Mater.* **2006**, *16*, 1799–1804.
- (19) An, B. K.; Kwon, S. K.; Park, S. Y. *Angew. Chem., Int. Ed.* **2007**, *46*, 1978–1982.
- (20) Briks, J. B. *Photophysics of Aromatic Molecules*; Wiley: London, 1970; pp 528–537.

Self-Assembly Morphology of CN-TFMBE Analogues with Functional Group Deficiencies. A slight structural modification in a π -electronic molecule can markedly affect its molecular packing or arrangement behavior, which may change the supramolecular architecture of organic solids.^{21,22} Therefore, to examine the structural origin of the ability of CN-TFMBE molecules to form highly fluorescent 1D-NWs, we designed and synthesized a series of reference CN-TFMBE analogues, which lack specific functional groups (CN or CF₃). These analogues included *trans*-4,4'-diphenylstilbene (DPST), *trans*-4,4'-di(3,5-bis-trifluoromethyl-phenyl)stilbene (TF-DPST), 2,3-bis-biphenyl-4-yl-acrylonitrile (CN-DPST), and 1-cyano-*trans*-1,2-bis-(3',5'-bis-methyl-biphenyl)ethylene (CN-BMBE), which has CH₃ end groups instead of CF₃. As seen in Figure 2, none of these analogue molecules with CN and/or CF₃ group deficiencies exhibited a 1-D NW morphology: DPST, TF-DPST, and CN-DPST show crystalline morphologies. Moreover, DPST, TF-DPST, and CN-DPST exhibit blue-shifted UV/vis absorption spectra (CN-TFMBE shows a red-shift from the isolated state to the aggregated state according to its *J*-stacking; see Supporting Information, Figure S1). These findings are consistent with our previous studies, which showed that the cyano group plays a significant role in inducing the head-to-tail type molecular arrangement.^{12,17,19,23} The present findings additionally show that the introduction of either a cyano group or CF₃ moieties alone into the backbone structure is not sufficient to induce 1D NW self-assembly.

Hierarchical Structure of Self-Assembled CN-TFMBE Molecules. In our earlier studies,^{11,12} we speculated on the basis of the observed optical properties that 1D-NW formation and the AIEE phenomenon arise from a synergistic effect between the planarization of molecules and the head-to-tail type *J*-stacking of CN-TFMBE molecules. To confirm this hypothesis in the present work and investigate the structural motif of CN-TFMBE molecules that gives rise to the facile formation of highly fluorescent 1D-NWs, we analyzed the self-assembled structure of CN-TFMBE 1D-NWs using mid- and wide-angle X-ray diffraction methods and multiscale computer simulation techniques.

As shown in Figure 3, the experimentally observed X-ray diffraction profiles (red dots) are in good agreement with the simulated profiles (blue line) in both the mid-angle (Figure 3a) and wide-angle regions (Figure 3b). The simulated profiles were obtained from the hierarchical self-assembled structure of CN-TFMBE molecules schematically shown in Figure 3e and f. To determine the self-assembled structure, possible assembly structure candidates were initially generated using an ab initio structure determination method based on the Monte Carlo/simulated annealing (MC/SA) methods, which are known to be useful in finding a structure without X-ray or other experimental data,^{24,25} and the final structure was then deter-

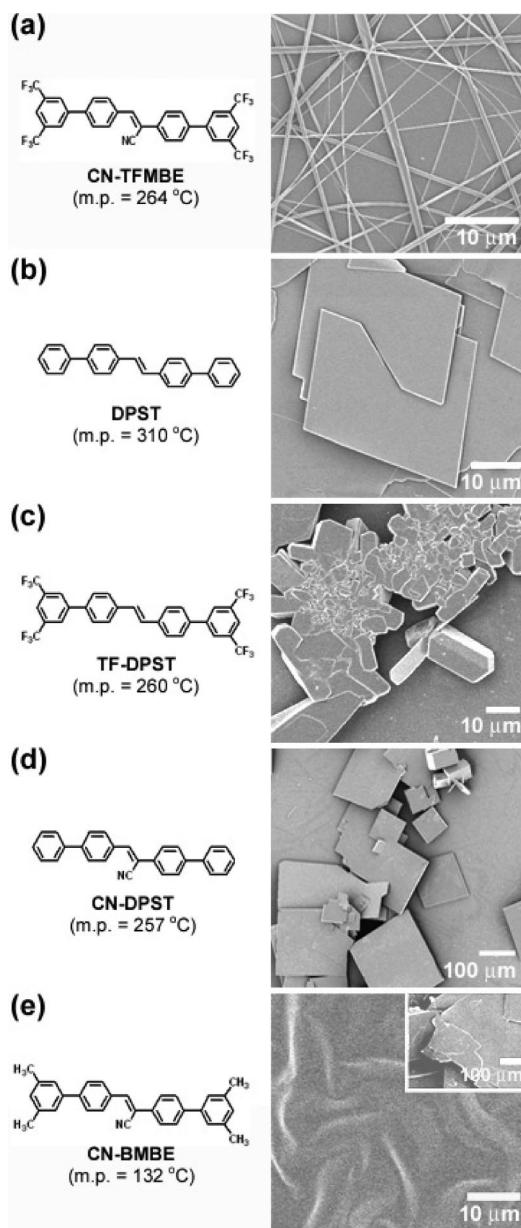


Figure 2. FE-SEM micrographs of (a) CN-TFMBE (1D wire structure), (b) DPST (3D crystal structure), (c) TF-DPST (3D crystal structure), (d) CN-DPST (3D crystal structure), and (e) CN-BMBE (amorphous film) fabricated by solution drop casting (0.2 wt % in 1,2-dichloroethane) onto a glass substrate. The inset photo in (e) shows the crystal morphology of CN-BMBE obtained by recrystallization from a dichloromethane/methanol mixture.

mined through iterative comparison-and-refinement procedures between experimental and simulated X-ray profiles (see the CIF file in Supporting Information).

From the mid-angle X-ray diffractogram of the aligned CN-TFMBE NWs (see Supporting Information, Figures S2 and S3) and the corresponding simulated most probable structures, it was found that each 1D-NW of CN-TFMBE molecules (Figure 3c) consists of a few nanofibril-like structural entities (denoted nanofibrils) oriented along the axis of the NW (Figure 3d). This can be confirmed from 2D X-ray pattern analysis in the mid-angle region (see Supporting Information, Figure S4). In addition, analysis of the wide-angle diffractogram (Figure 3b) indicates that the nanofibril-like structural entities are formed by the lengthwise stacking (i.e., head-to-tail type *J*-stacking)

- (21) Bartholomew, G. P.; Bazan, G. C.; Bu, X. H.; Lachicotte, R. J. *Chem. Mater.* **2000**, *12*, 1422–1430.
- (22) Velde, C. M. L. V.; Chen, L. J.; Baeke, J. K.; Moens, M.; Dieltiens, P.; Geise, H. J.; Zeller, M.; Hunter, A. D.; Blockhuys, F. *Cryst. Growth Des.* **2004**, *4*, 823–830.
- (23) Oelkrug, D.; Tompert, A.; Gierschner, J.; Egelhaaf, H. J.; Hanack, M.; Hohloch, M.; Steinhuber, E. *J. Phys. Chem. B* **1998**, *102*, 1902–1907.
- (24) Verwer, P.; Leusen, F. J. J. *Computer Simulation to Predict Possible Crystal Polymorphs in Reviews in Computational Chemistry*; Lipkowitz, K. B., Boyd, D. B., Eds.; Wiley-VCH: New York, 1998; Vol. 13, pp 327–365.
- (25) Motherwell, W. D. S.; et al. *Acta Crystallogr., Sect. B* **2002**, *58*, 647–661.

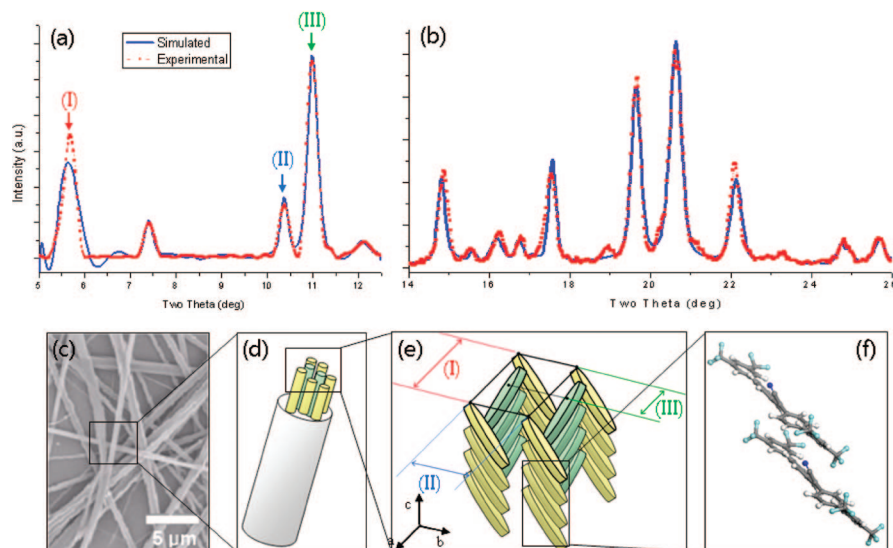


Figure 3. Simulated (blue solid line) and experimental (red dots) X-ray profiles in the (a) midangle and (b) wide-angle regions. (c) SEM micrograph of 1D-NWs. (d) Schematic of a 1D-NW consisting of nanofibril-like structural entities. (e) Schematic of the molecular self-assembled structure within the nanofibril-like structural entities. The interfibrillar spacings (I) (red), II (blue) and III (green)) are determined from the peak positions in the midangle X-ray profile in (a). (f) Final energy-minimized and structurally optimized bimolecular stacking structure extracted from (e).

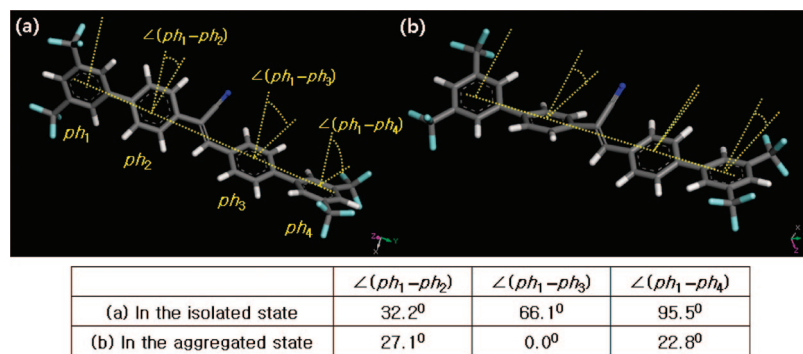


Figure 4. Molecular conformations (a) before and (b) after self-assembly of CN-TFMBE molecules. Each torsion angle $\angle \text{Ph}_1-\text{Ph}_j$ was measured relative to the plane of the leftmost phenyl ring (Ph_1).

of anisotropic CN-TFMBE molecules (Figure 3f). It is also worthwhile to note that the normal of CN-TFMBE molecules changes alternatively in opposite ways, i.e. symmetrically for the axis of 1D-NWs, from one nanofibril to another (Figure 3e).

Conformation Change of CN-TFMBE Molecules during the Self-Assembly Process. Another interesting and very important observation from both the wide-angle X-ray profiles (Figure 3b) and the final self-assembled structure (Figure 3f and Figure S5 in Supporting Information) is that the conformation of the CN-TFMBE molecules changes during the self-assembly process. Indeed, comparison of the molecular conformations in the aggregated state (Figure 3f) and isolated state reveals that the torsion angles ($\angle \text{Ph}_1-\text{Ph}_j$) between the first (Ph_1) and the other phenyl ring planes (Ph_j , $j = 2, 3, 4$) differ considerably. As shown in Figure 4, in the isolated state, the phenyl rings are significantly distorted from each other so that the torsion angle of $\angle \text{Ph}_1-\text{Ph}_4$ reaches up to 95.5° (Figure 4a), but in the aggregated state the phenyl rings are flattened (denoted as coplanarization); consequently, the torsion angle of $\angle \text{Ph}_1-\text{Ph}_4$ is reduced to 22.8°. In particular, the first and third phenyl rings are coplanar in the aggregated state (i.e., the torsion angle $\angle \text{Ph}_1-\text{Ph}_3$ is 0°; Figure 4b).

To further explore this conformation change during self-assembly, we calculated the changes in both the total energy and its component energies of the self-assembly system, that is, the intramolecular and intermolecular interaction energies. The total energy, calculated on the assumption that the distorted molecules (i.e., the molecules in the isolated state) were packed into the as-determined final self-assembled structure (Case 1), was found to be about 4,000,000 kcal/mol, whereas that of the planarized molecules that are in the structurally optimized and energetically minimized final assembled structure was 122 kcal/mol. This striking difference in total energy indicates that the coplanarization of the phenyl rings in the CN-TFMBE molecule is the key thermodynamic factor driving the self-assembly process. When the intermolecular distances are released and hence the molecular positions are released but the molecular conformations are fixed (Case 2), the total energy shows more rational value, but the structure and its simulated X-ray profile are quite different from the experimental value (see Supporting Information, Figure S6). On the basis of this observation and the calculation of molecular interaction energies as a function of the intermolecular distance, we can deduce the self-association behavior of CN-TFMBE molecules, as shown in Figure 5. The presence of the polar cyano group on the backbone structure increases the polarity of the molecules, resulting in

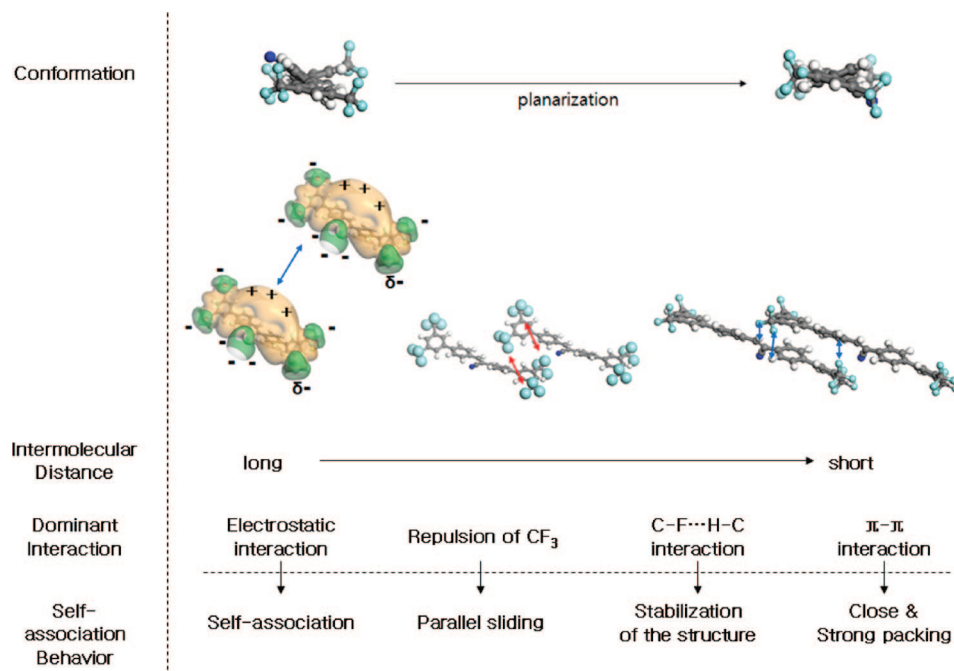


Figure 5. Scheme for conformation changes, dominant interactions, and the self-association behavior of CN-TFMBE molecules with varying the intermolecular distances.

an anisotropic electronic distribution (see Supporting Information, Figure S7), thus strengthening the electrostatic interaction between neighboring molecules. As a result, the molecules experience a long-range attraction despite the presence of bulky and repulsive CF_3 end groups. As the molecules approach one another, the phenyl rings in the backbone structure begin to become planarized to maximize the interaction, but because of the repulsion induced by the bulky CF_3 groups, the approaching molecules tend to slide away along the molecular axis. However, this repulsive molecular movement is stabilized by compensating energetic contributions arising from $\text{C}-\text{F}\cdots\text{H}-\text{C}$ hydrogen bonding and the partially overlapped $\pi-\pi$ interaction of the neighboring phenyl rings. Here, $\text{C}-\text{F}\cdots\text{H}-\text{C}$ hydrogen bonding denotes a specific interaction between highly electronegative fluorine atoms in trifluoromethyl units and the hydrogen atoms in phenyl rings of the neighboring molecules. It is well-known that $\text{C}-\text{F}\cdots\text{H}-\text{C}$ type hydrogen bonds are major interactions stabilizing molecular assembled structures when stronger interactions such as $\text{O}-\text{H}$ hydrogen bonds are absent.^{26–29} In addition, the importance of such interactions is suggested by our observation that CN-BMBE molecules (see Figure 2e), which have CH_3 end groups and hence cannot form $\text{C}-\text{F}\cdots\text{H}-\text{C}$ type hydrogen bonds, do not form 1D NWs and exhibit a much lower melting temperature of 132 °C compared to their counterparts with CF_3 end groups (i.e., CN-TFMBE molecules).

Taking together the above-mentioned observations and discussions, we conclude that the easy formation of 1D-NWs and the AIEE of self-assembled CN-TFMBE molecules are fundamentally due to the relative contributions of various kinds of

intermolecular interactions. In view of the molecular structure, the presence of a CN group and CF_3 end groups induces the planarization of the CN-TFMBE molecules and hence head-to-tail type *J*-aggregation during the self-assembly process, which leads to greatly enhanced AIEE.

Color-Tuned Highly Fluorescent 1D-NWs and Nanofabrics (2D-NFs). On the basis of the molecular structure guidelines for the easy formation of highly fluorescent 1D-NWs, which include the high polarity induced by the cyano group, the energy balance between steric repulsion and hydrogen bonding associated with the CF_3 end groups, and the planarity of the backbone phenyl rings, we can design and prepare new color-tuned highly fluorescent 1D-NWs, such as THIO-G, THIO-Y and DM-R (Figure 6), in addition to the highly blue fluorescent CN-TFMBE 1D-NWs (Figure 6e). During the course of the chemical synthesis and purification processes, these newly designed molecules, which are analogues of CN-TFMBE, easily formed a bundle of 1D-NWs to yield a pulp-like morphology (see Supporting Information, Figure S8) that has rarely been observed in conventional OPV molecular systems. Indeed, FE-SEM micrographs (Figure 6b–d) of THIO-G, THIO-Y, and DM-R 1D-NWs prepared by solution casting of a 0.5 wt % solution in 1,2-dichloroethane/methanol (9:1 v/v) reveal that the ultralong 1D-NWs with minimum diameters of about 100 nm are bundled and populated over a large area of the substrate without any other impurities (1D structural defects).

The THIO-G, THIO-Y, and DM-R 1D-NWs exhibited well-defined fluorescent emission colors, i.e., green ($\lambda_{\text{max}} = 543$ nm, CIE = x (0.35), y (0.60)), yellow ($\lambda_{\text{max}} = 564$ nm, CIE = x (0.44), y (0.55)), and red ($\lambda_{\text{max}} = 598$ nm, CIE = x (0.53), y (0.47)) fluorescent colors, respectively (see Figure 6e–h) and Supporting Information, Figure S9). Also, these color-tuned 1D-NWs exhibited much enhanced fluorescence emission (THIO-G ($I_{\text{A/I}} = 163.0$), THIO-Y ($I_{\text{A/I}} = 5.0$), and DM-R ($I_{\text{A/I}} = 2.1$)) with the red-shift of emission spectra from the isolated molecular state (I) to the aggregated state (A) due to the combined effects

- (26) Shimon, L.; Carrell, H. L.; Glusker, J. P.; Coombs, M. M. *J. Am. Chem. Soc.* **1994**, *116*, 8162–8168.
- (27) Boitsov, S.; Songstad, J.; Tornroos, K. W. *Acta Crystallogr.* **2002**, *C58*, o66–o68.
- (28) Emmerling, F.; Orgzall, I.; Dietzel, B.; Schulz, B. W.; Reck, G.; Schulz, B. *J. Mol. Struct.* **2007**, *832*, 124–131.
- (29) Kim, H. I.; Koini, T.; Lee, T. R.; Perry, S. S. *Langmuir* **1997**, *13*, 7192–7196.

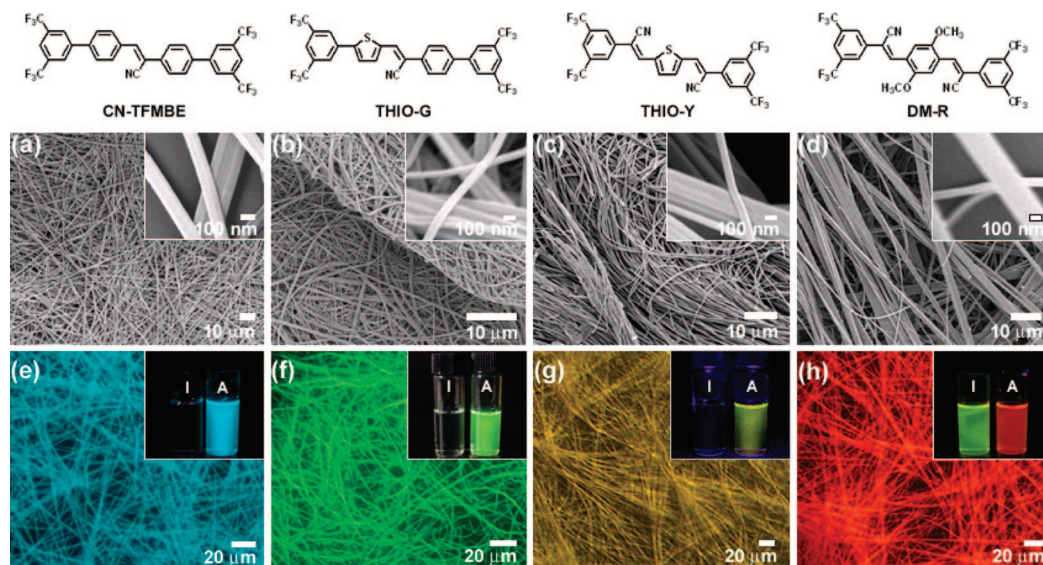


Figure 6. (a–d) SEM micrographs of CN-TFMBE, THIO-G, THIO-Y, and DM-R NWs generated by solution drop casting (0.5 wt % in 1,2-dichloroethane/methanol (9:1 v/v)), respectively. (e–h) Fluorescence microscopy images of CN-TFMBE, THIO-G, THIO-Y, and DM-R NW structures generated by the method described for (a–d), respectively. Inset photos show the fluorescence colors of the isolated molecular state in THF solution (I) and the aggregated nanoparticle state in THF/water (1:4 v/v) (A), respectively. The concentration of all solutions is 2×10^{-5} mol/L.

of aggregation-induced planarization and *J*-aggregate formation, the so-called AIEE phenomenon (see Figure 6f–h) inset photos and Supporting Information, Figure S10 and S11).

Other interesting characteristics of these color-tuned highly fluorescent 1D-NWs are that they can easily form mechanically stable 2D nonwoven nanofabrics (2D-NFs) in large amounts when the dye concentration in the solution exceeds 2.0 wt % and can show the fairly high photoluminescence quantum yield (PLQY) in the solid state. It was found that the PLQY of the 2D-NFs of CN-TFMBE, THIO-G, THIO-Y, and DM-R show the 93.9% (91.7 %),³⁰ 22.5%, 15.3%, and 9.5%, respectively. Furthermore, these highly fluorescent 2D-NFs could readily be shaped into various desired forms with active areas ranging from ~ 0.3 cm² to ~ 1.2 cm² by molding or stamping techniques (Figure 7a). It should also be noted that the surfaces of the 2D-NFs are highly hydrophobic, as demonstrated by their contact angles (~ 110 – 137° ; Figure 7a). Compared to the contact angles of general hydrophobic films of π -electronic molecules ($<110^\circ$)^{31,32} and untreated polytetrafluoroethylene (PTFE, $<105^\circ$),³³ the surfaces of the 2D-NFs are remarkably hydrophobic; in particular, the DM-R 2D-NF surfaces exhibited contact angles that are very close to those of superhydrophobic surfaces that have the contact angles normally higher than 150° .³⁴ The high hydrophobicity of the color-tuned 2D-NF surfaces is highly advantageous in their practical applications because π -electronic molecules, and the performance of devices based on such molecules, are influenced significantly by environmental exposure to moisture, which generally causes chemical degradation and a sharp decrease in physical stability.^{35,36}

Another noteworthy feature is that, when we adopted a modified soft deposition technique,³⁷ a thicker fabric consisting of multiple layers of different kinds of 2D-NFs could be obtained. Such heterogeneous multilayered 2D-NFs are known to be difficult to fabricate, in cases of general multilayer films or assemblies of π -electron molecules, by solution processes such as drop-casting and spin-coating techniques. This is because the predeposited layer is dissolved and eliminated during the deposition of the second layer. However, as shown in Figure 7b, we successfully fabricated composite 2D-NFs consisting of three layers, one each of CN-TFMBE (blue emission, ~ 20 μ m thickness), THIO-Y (green emission, ~ 20 μ m thickness), and DM-R (red emission, ~ 30 μ m thickness), in sequence without breaking the 1D-NW structures (Figure 7b inset SEM micrographs). It was also found that the thick 2D-NFs had excellent mechanical properties (see Supporting Information, Figure S12) such that they were self-supportable and had excellent flexibility (Figure 7c). Furthermore, due to the outstanding flexibility of the 2D-NFs, it was possible to fabricate 2D-NFs even on curved substrates. Figure 7d shows a spherical substrate of volume $\sim 36\pi$ mm³ that is entirely wrapped by a layer of CN-TFMBE 2D-NFs of thickness ~ 10 μ m. Similar to the other cases, the individual NWs in the CN-TFMBE 2D-NFs remain intact even on the curved surface of the ball (FE-SEM images in Figure 7d). We expect that our color-tuned highly fluorescent 2D-NFs will enhance the performance and extend the characteristic functions of 1D-NWs for many technological optoelectronic and sensing applications.^{38–41}

Conclusions

Through systematic analyses of the self-assembled structure and self-association behavior of CN-TFMBE and its analogues

(30) The absolute PLQYs of the CN-TFMBE NW fabrics were cross-checked with two separate laboratories.

(31) Seferos, D. S.; Banach, D. A.; Alcantar, N. A.; Israelachvili, J. N.; Bazan, G. C. *J. Org. Chem.* **2004**, *69*, 1110–1119.

(32) Robinson, L.; Isaksson, J.; Robinson, N. D.; Berggren, M. *Surf. Sci.* **2006**, *600*, L148–L152.

(33) Kim, S. R. *J. Appl. Polym. Sci.* **2000**, *77*, 1913–1920.

(34) Li, X. M.; Reinhoudt, D.; Crego-Calama, M. *Chem. Soc. Rev.* **2007**, *36*, 1350–1368.

(35) Czerwinski, A.; Cunningham, D. D.; Amer, A.; Schrader, J. R.; Vanpham, C.; Zimmer, H.; Mark, H. B.; Pons, S. *J. Electrochem. Soc.* **1987**, *134*, 1158–1164.

(36) Hoshino, S.; Yoshida, M.; Uemura, S.; Kodzasa, T.; Takada, N.; Kamata, T.; Yase, K. *J. Appl. Phys.* **2004**, *95*, 5088–5093.

(37) Shimizu, K. T.; Tabbri, J. D.; Jelincic, J. J.; Melosh, N. A. *Adv. Mater.* **2006**, *18*, 1499–1504.

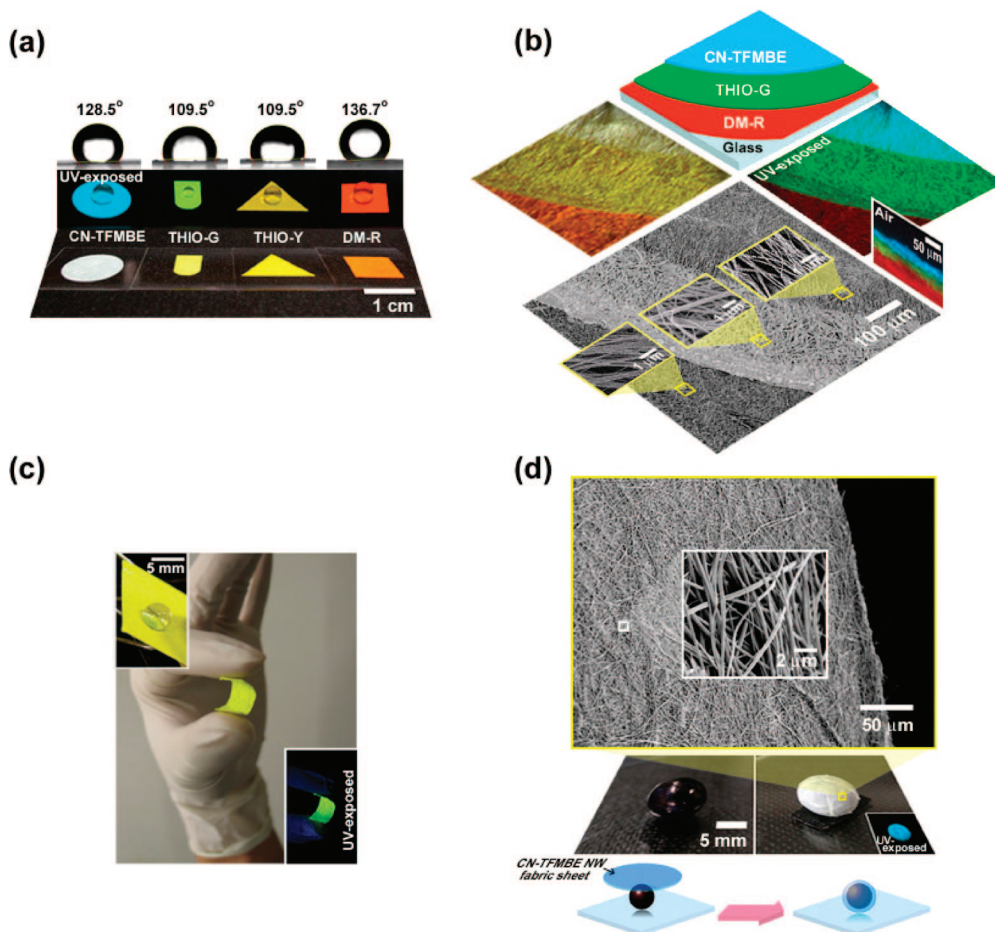


Figure 7. (a) Photo and fluorescence images of CN-TFMBE (blue), THIO-G (green), THIO-Y (yellow), and DM-R (red) 2D-NFs with various shapes. The black-and-white photo shows the contact angle of a water drop on each 2D-NF. (b) Fluorescence microscopy and SEM images of multilayer structures of CN-TFMBE, THIO-G, and DM-R 2D-NFs deposited on glass substrates without wrinkling. The vertical fluorescence microscopy image shows the cross section of the multilayers of the 2D-NFs ($\sim 100\ \mu\text{m}$) and fluorescence image of the curved form (lower inset). (c) Flat (upper inset) and curved form of the THIO-G 2D-NFs ($\sim 100\ \mu\text{m}$) and fluorescence image of the curved form (lower inset). (d) Photo and SEM images of the CN-TFMBE 2D-NFs deposited on a plastic ball substrate (a volume of $36\pi\ \text{mm}^3$).

using mid- and wide-angle X-ray diffraction and multiscale computer simulation techniques, we successfully formulated molecular structural guidelines for the easy and massive formation of highly fluorescent 1D-NWs. It was found that the cyano group on the backbone of CN-TFMBE serves to increase the polarity of the molecule and to give rise to an anisotropic electronic distribution, leading to stronger intermolecular Coulombic interactions. The π - π interaction between nearest-neighbor molecules seems to be strengthened by coplanarization of the phenyl rings when the molecules are in close proximity. The bulky CF_3 groups attached to the phenyl rings at each end of CN-TFMBE give rise to a sliding of the molecules along the molecular axis direction and the formation of hydrogen bonding of the type $\text{C}-\text{F}\cdots\text{H}-\text{C}$. The formation of 1D-NWs of CN-TFMBE molecules was found to result from the relative contributions of these three major interactions to the intermolecular distances, arising intrinsically from the aforementioned structural factors. On the basis of these structural guidelines, we successfully prepared highly fluorescent color-tuned 1D-

NWs and 2D-NFs. These new nanomaterials exhibited well-defined optical properties and excellent mechanical stabilities. In addition, our new compounds readily formed 1D-NWs and/or 2D-NFs, irrespective of the processing method and conditions used. This class of highly fluorescent color-tuned organic π -electronic nanomaterials is expected to open a new phase in applications such as nanoscale optoelectronics, sensors, and biological devices.

Experimental Section

Methods and Instrumentation. All chemicals were purchased from Aldrich or Lancaster Co. DPST was purchased from Lancaster Co. and used without further purification. CN-TFMBE and CN-BMBE were synthesized according to the method described in our previous paper.¹¹ The synthetic routes and characterizations of TF-DPST, CN-DPST, THIO-G, THIO-Y, and DM-R are described in the Supporting Information. ^1H NMR spectra were recorded on a Jeol JNM-LA300 (300 MHz) spectrometer in CDCl_3 solution with CHCl_3 at 7.26 ppm as the internal standard. IR spectra were measured on a Midac FT-IR spectrophotometer using KBr pellets. Mass spectra were measured on a JMS AX505WA instrument in EI or FAB mode. UV-visible absorption and fluorescence emission spectra were recorded on HP 8452-A and Shimadzu RF-500

(38) Service, R. F. *Science* **2003**, *301*, 909–911.

(39) Hamed, M.; Forchheimer, R.; Inganas, O. *Nat. Mater.* **2007**, *6*, 357–362.

(40) Abouraddy, A. F.; Bayindir, M.; Benoit, G.; Hart, S. D.; Kuriki, K.; Orf, N.; Shapira, O.; Sorin, F.; Temelkuran, B.; Fink, Y. *Nat. Mater.* **2007**, *6*, 336–347.

(41) Staneva, D.; Betcheva, R.; Chovelon, J. M. *J. Appl. Polym. Sci.* **2007**, *106*, 1950–1956.

spectrofluorophotometers, respectively. FE-SEM and TEM images were acquired on JSM-6330F (JEOL) and JEM-2200FS (JEOL) instruments, respectively. The melting temperatures of all compounds were determined by differential scanning calorimetry (Perkin-Elmer DSC-7). Fluorescence images were obtained using a digital camera (Nikon-Coolpix 995) and a microscope (Leica) under illumination at 365 nm. The optimized geometry and electron density of the synthesized molecules in the gas phase were calculated using the AM1 parametrization in the HyperChem 5.0 program (Hypercube). The contact angles were measured using a Phoenix 150 contact angle analyzer (S.E.O.) with image XP software. Static contact angle measurements were carried out 60 s after the droplet was deposited on the surface. Measurements of five droplets of 10 μL of distilled water were averaged. Mid-angle X-ray diffractometry was carried out using Cu K α radiation focused by cross-coupled Göbel mirrors on a Nanostar (Bruker) instrument equipped with a High Star 2D area detector, operating at 40 kV and 35 mA. Wide-angle X-ray diffractograms were acquired in reflection mode using Ni-filtered Cu K α radiation on a D8 Advance (Bruker) instrument equipped with a point detector, operating at 40 kV and 40 mA. Computer simulations were carried out using the MS Modeling 4.0 Software package (Accelrys). The "Polymorph" module was used for ab initio structure determination, the "Discover" and "Forcite" modules for force field-based energy calculation, and the "DMol3" module for quantum chemistry calculations. For the measurement of absolute photoluminescence quantum yield of the nanowire fabric structures, a He/Cd CW laser was used to excite the sample placed in the sphere with $\lambda = 325$ nm as the excitation wavelength. The absolute photoluminescence quantum efficiency of the nanowire fabric structure was measured using an integrating sphere (Labsphere Co., 600 nm diameter) as described in the literature.⁴² A continuous wave He/Cd laser ($\lambda = 325$ nm, Mellisgriot Co.) was used as the excitation light source, and a monochromator (Acton Research Co.) attached with a photomultiplier tube (Hamamatsu) was used as the optical detector system. The laser was irradiated from the quartz side, and its power was adjusted to less than 2 mW/cm² to prevent damage to the samples. Excitation beam size was adjusted to have 1 cm in diameter. All the systems were calibrated by using tungsten-halogen standard lamp and deuterium lamp (Ocean Optics LS-1-CAL and DH-2000-CAL, respectively). For system verification we have measured the PL efficiency of well-known materials, such as 9,10-diphenylanthracene, fluorescence in 0.1 N sodium hydroxide, coumarin 102, Rhodamine B, and tris(8-hydroxyquinoline) aluminum. All results had reliable values with the reported one within $\pm 3\%$. To avoid sample degradation by laser excitation, the samples were kept in an inert environment by blowing nitrogen gas into the integrating sphere.

Fabrication of CN-TFMBE 1D-NWs in a PMMA Matrix.

Thermal Annealing Method. A CN-TFMBE-doped polymer film was spin coated (2500 rpm, film thickness = approximately 200 nm) from a filtered 3.0 wt % solution of CN-TFMBE (10.0 wt % with respect to PMMA) and poly(methyl methacrylate) (PMMA,

average MW = 120,000) in 1,2-dichloroethane. Initially, the spin-coated film was smooth and uniform without any discernible nanosized objects. After annealing the film at 65 °C for 45 min, however, the annealed film was found to exhibit very slight off-white turbidity due to the formation of CN-TFMBE 1D-NWs.

VDSA Method.¹⁹ A CN-TFMBE-doped polymer film was prepared by the method described above. The fabricated film was then turned upside down and placed on top of the spout of a 20 mL vial in which 1 mL of 1,2-dichloromethane (DCM, vapor pressure (vp) = 6.83 psi (20 °C)) was added at room temperature over about 30 s. After exposing the film to DCM vapor for 30 s, the vapor-exposed region of the film exhibited drastic fluorescence emission color changes from blue emission to sky-blue emission due to the AIEE phenomenon induced by the generation of CN-TFMBE NW aggregates.

Fabrication of Nanoparticle Suspension Solutions for the Study of the Molecular Packing in the Dye Aggregated State.

Nanoparticle suspensions were prepared by a reprecipitation method (using the Ouzo effect); 4 mL of distilled water was regularly injected into the dye solution in THF (1 mL) with vigorous stirring at room temperature, using a syringe pump. Before the injection of the distilled water, the distilled water and the dye solution were filtered through a membrane filter with a pore size of 0.2 μm .

Fabrication of Various Shaped NW Fabric Sheets. Molding method (CN-TFMBE): Dye solutions (>2 wt %) in 1,2-dichloroethane or methanol/1,2-dichloroethane mixtures were dropped inside a circle-shaped mold installed on a glass substrate. The dye solutions were then slowly dried at room temperature, after which the mold was carefully removed.

Stamping method (THIO-G, THIO-Y and DM-R): The same dye solutions were dropped onto a glass substrate, and slowly dried at room temperature to prepare NW fabric sheets. The unwanted parts of the original random-shaped NW fabric sheets were cut out using stamps (THIO-G) or cutters (THIO-Y and DM-R) to produce specific patterns.

Fabrication of Multilayer NW Fabric Sheets and Deposition of CN-TFMBE NW Fabric Sheets onto a Spherical Substrate. The detailed procedures are described in the Supporting Information, (Figures S13 and S14).

Acknowledgment. This work was supported by the Korea Science and Engineering Foundation (KOSEF) through the National Research Laboratory Program funded by the Ministry of Science and Technology (No.2006-03246), Center for Electro-Photo Behaviors in Advanced Molecular Systems (R11-2008-052-01003) and the Korea Foundation for International Cooperation of Scientific and Technology (KICOS) through a grant provided by the Korea Ministry of Education, Science and Technology (MEST) (K20704000008).

Supporting Information Available: Synthesis and characterization data (¹H NMR, FT-IR, and mass spectra, elementary analysis, and optical data of compounds) and details of the structural study. Complete ref. This material is available free of charge via the Internet at <http://pubs.acs.org>.

JA806162H

- (42) (a) de Mello, J. C.; Wittmann, H. F.; Friend, R. H. *Adv. Mater.* **1997**, *9*, 230–232. (b) Pålsson, L.-O.; Monkman, A. P. *Adv. Mater.* **2002**, *14*, 757–758. (c) Babu, S. S.; Praveen, V. K.; Prasanthkumar, S.; Ajayagosh, A. *Chem. Eur. J.* **2008**, *14*, 9577–9584.